Inorg. Chem. **2002**, *41*, 3375–3384

Synthesis, Structures, and Magnetic Properties of a Series of Lanthanum(III) and Gadolinium(III) Complexes with Chelating Benzimidazole-Substituted Nitronyl Nitroxide Free Radicals. Evidence for Antiferromagnetic Gd^{III}–Radical Interactions

Christophe Lescop,[†,‡] Elie Belorizky,[§] Dominique Luneau,*[,†] and Paul Rey[†]

Laboratoire de Chimie Inorganique et Biologique (UMR 5046), DRFMC, CEA-Grenoble, 17 rue des Martyrs, 38054 Grenoble Cedex 09, France, and Laboratoire de Spectrométrie Physique (UMR 5588), Université Joseph Fourier, Grenoble 1, BP 87, 38402 Saint Martin d'Hères, France

Received January 2, 2002

This paper reports the synthesis, crystal structures, and magnetic properties of a series of lanthanide complexes with nitronyl nitroxide radicals of general formula $\{[Ln^{III}(radical)_4]\cdot(ClO_4)_3\cdot(H_2O)_x\cdot(THF)_y\}$ (**1**–**4**) and $[Ln^{III}(radical)_2(NO_3)_3]$ (**5**, **6**) [Ln = La (compounds **1**, **3**, **5**) or Gd (compounds **2**, **4**, and **6**); radical = 2-(2′-benzymidazolyl)-4,4,5,5-tetramethylimidazoline-1-oxyl-3-oxide (**NITBzImH**, compounds **1**, **2**, **5**, **6**) or 2-{2′-[(6′-methyl)benzymidazolyl]}-4,4,5,5-tetramethylimidazoline-1-oxyl-3-oxide (**NITMeBzImH**, compounds **3**, **4**)]. **(1)** $C_{64}H_{88}Cl_3LaN_{16}O_{24}$, fw = 1710.76, orthorhombic, *Fddd*, a = 11.0682(8) Å, b = 34.240(3) Å, c = 42.787(3) Å, V = 16215(2) Å^3, Z = 8, R = 0.0876, R_w = 0.2336. **(2)** $C_{64}H_{88}Cl_3GdN_{16}O_{24}$, fw = 1729.10, tetragonal, $P\bar{4}2c$, a = 16.0682(4) Å, b = 16.0682(4) Å, c = 18.7190(6) Å, V = 4833.0(2) Å^3, R = 0.0732, R_w = 0.2218. **(3)** $C_{68}H_{94}Cl_3LaN_{16}O_{23}$, fw = 1742.80, tetragonal, $P\bar{4}2_1m$, a = 21.125(3) Å, b = 21.125(3) Å, c = 10.938(2) Å, V = 4881.5(14) Å^3, R = 0.1017, R_w = 0.3126. **(5)** $C_{28}H_{34}LaN_{11}O_{13}$, fw = 871.57, orthorhombic, $Pna2_1$, a = 19.5002(12) Å, b = 13.0582(8) Å, c = 14.5741(9) Å, V = 3711.1(4) Å^3, R = 0.0331, R_w = 0.1146. **(6)** $C_{28}H_{34}GdN_{11}O_{13}$, fw = 889.91, orthorhombic, $Pna2_1$, a = 19.1831(10) Å, b = 13.1600(7) Å, c = 14.4107(7) Å, V = 3638.0(3) Å^3, Z = 4, R = 0.0206, R_w = 0.0625. Compounds **1**–**4** consist of $[M^{III}(radical)_4]^{3+}$ cations, uncoordinated perchlorate anions, THF, and water crystallization molecules. In these complexes, the coordination number around the lanthanide ion is eight, and the polyhedron is either a distorted dodecahedron (**1**) or a distorted cube (**2**, **3**). The crystal structures of **5** and **6** consist of independent $[M^{III}(radical)_2(NO_3)_3]$ entities in which the lanthanide is ten-coordinated and has a distorted bicapped square antiprism coordination polyhedron. For the lanthanum(III) complexes, the temperature dependence of the magnetic susceptibility indicates that radical–radical magnetic interactions are negligible either for compounds **1** and **3**, while for compound **5** it is simulated considering dimers of weakly antiferromagnetically coupled radicals ($J_{rad-rad}$ = –1.1 cm^{-1}). In the case of the gadolinium(III) compounds (**2**, **4**, **6**), each magnetic behavior gives unambiguous evidence of antiferromagnetic Gd^{III}–radical interaction (**2**, J_{Gd-rad} = –1.8 cm^{-1}; **4**, J_{Gd-rad} = –3.8 cm^{-1}; **6**, $J_{Gd-rad1}$ = –4.05 cm^{-1} and $J_{Gd-rad2}$ = –0.80 cm^{-1}), in contrast to the ferromagnetic case generally observed. The nature of the Gd^{III}–radical interaction is explained in relation to the donor strength of the free radical ligand.

Introduction

On the basis of numerous studies, the magnetic coupling between gadolinium(III) and free radicals,[1−5] or copper(II)[6−15] and vanadyl(II) metal ions,[13] has long been considered to be ferromagnetic, independent of any structural parameters

* To whom correspondence should be addressed. E-mail: luneau@drfmc.ceng.cea.fr.

† Laboratoire de Chimie Inorganique et Biologique (UMR 5046), DRFMC.

‡ Present address: Organométalliques et Catalyse: Chimie et Electrochimie Moléculaires, UMR 6509, Institut de Chimie de Rennes, CNRS-Université de Rennes 1, Campus de Beaulieu, 35042 Rennes Cedex, France.

§ Laboratoire de Spectrométrie Physique (UMR 5588), Université Joseph Fourier.

(1) Benelli, C.; Caneschi, A.; Gatteschi, D.; Pardi, L.; Rey, P. *Inorg. Chem.* **1990**, *29*, 4223.
(2) Benelli, C.; Caneschi, A.; Gatteschi, D.; Pardi, L.; Rey, P. *Inorg. Chem.* **1989**, *28*, 275.
(3) Benelli, C.; Caneschi, A.; Gatteschi, D.; Pardi, L. *Inorg. Chem.* **1992**, *31*, 741.
(4) Benelli, C.; Caneschi, A.; Gatteschi, D.; Laugier, J.; Rey, P. *Angew. Chem., Int. Ed. Engl.* **1987**, *26*, 913.
(5) Sutter, J.-P.; Kahn, M. L.; Golhen, S.; Ouahab, L.; Kahn, O. *Chem.—Eur. J.* **1998**, *4*, 571.

10.1021/ic0200038 CCC: $22.00
Published on Web 06/06/2002

or ligand effects. This was well explained as the result of electron transfer from the free radical, or from the transition metal magnetic orbitals (3d), into the empty gadolinium(III) orbitals, either the 5d or the 6s, that stabilizes the ground state with the higher spin multiplicity owing to Hund's rule.[8,11] Confidence in these models relied on the fact that any antiferromagnetic couplings which could arise from overlap involving the 4f magnetic orbitals of gadolinium(III) are excluded as a consequence of the low spatial expansion of the 4f orbitals.

However, our first finding of antiferromagnetic Gd^{III}−radical interactions in nitronyl nitroxide complexes,[16] followed by other evidence of Gd^{III}−radical and $Gd^{III}-Cu^{II}$ antiferromagnetic couplings,[17,18] has greatly unsettled the confidence that Gd^{III}−radical or $Gd^{III}-Cu^{II}$ is intrinsically ferromagnetic. With the aim to support our first results, we undertook the synthesis and magnetic studies of lanthanide(III) complexes with chelating nitronyl nitroxide radicals, varying the donor strength and the number of radical ligands, or the coordination geometry around the metal center. The lanthanum analogues were also synthesized in order to evidence the radical−radical interactions.

We report herein the synthesis, crystal structures, and magnetic properties of three lanthanum(III) and three gadolinium(III) complexes of nitronyl nitroxide radicals substituted either by the 2-benzimidazolyl (**NITBzImH**) or the 2-(6-methylbenzimidazolyl) (**NITMeBzImH**) substituents (Figure 1). Some of these compounds were partly reported in previous communications.[16,19] All gadolinium(III) complexes exhibit antiferromagnetic Gd^{III}−radical interactions. These results suggest that the sign of the magnetic interaction should depend on structural and ligand effects.

Experimental Section

Syntheses. 2,3-Bis-(hydroxylamino)-2,3-dimethylbutane, 2-(2′-benzymidazolyl)-4,4,5,5-tetramethylimidazoline-1-oxyl-3-oxide (**NITBzImH**), and 2-{2′-[(6′-methyl)benzymidazolyl]}-4,4,5,5-tetramethylimidazoline-1-oxyl-3-oxide (**NITMeBzImH**) were prepared according to literature methods.[20,21] Other reactants were used as purchased. THF was distilled over sodium−potassium/benzophenone. **Safety Notes.** *Metal perchlorate containing organic ligands are potentially explosive. Only a small amount of material should be prepared, and it should be handled with great care.*

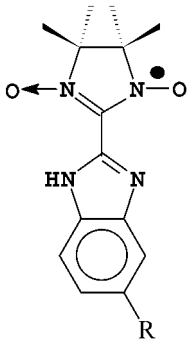

Figure 1. Schematic representation of the nitroxide radical R = H (radical **NITBzImH**, complexes **1**, **2**, **5**, **6**) and R = Me (radical **NITMeBzImH**, complexes **3**, **4**).

Compounds **1**−**6** are very stable, even those containing solvent of crystallization (water, THF). The perchlorate derivatives (**1**−**4**) were synthesized in THF. The success of growing single crystals depended drastically on the amount of water in THF, and anhydrous complexes were not characterized.

$[La^{III}(NITBzImH)_4]\cdot(ClO_4)_3\cdot 2THF\cdot 2H_2O$ (1), $[Gd^{III}(NITBzImH)_4]\cdot(ClO_4)_3\cdot 2THF\cdot 2H_2O$ (2), $[La^{III}(NITMeBzImH)_4]\cdot(ClO_4)_3\cdot 2THF\cdot 1H_2O$ (3), $[Gd^{III}(NITMeBzImH)_4]\cdot(ClO_4)_3\cdot 2THF\cdot 1H_2O$ (4). The four compounds were synthesized following a procedure similar to that exemplified for **1** hereafter. A 40 mg (0.073 mmol) portion of $La^{III}(ClO_4)_3\cdot 6H_2O$ was dissolved in 5 mL of anhydrous THF. To this solution were successively added 40 μL of water and 80 mg (0.3 mmol) of nitronyl nitroxide radical (**NITBzImH**) previously dissolved in 15 mL of anhydrous THF. The resultant blue-green solution was left uncovered in a desiccator. After 12 h, block shaped crystals started to form, and after 4 days, 40 mg (yield 32%) of dark blue crystals was isolated by filtration. In the case of compound **4**, trials to get single crystals suitable for X-rays diffraction studies failed.

Anal. Calcd (**1**) $C_{64}H_{88}N_{16}O_{24}Cl_3La$: C, 44.9; H, 5.2; N, 13.1; O, 22.5; Cl, 6.2; La, 8.1. Found: C, 44.9; H, 5.2; N, 13.1; Cl, 6.7; La, 7.5. Anal. Calcd (**2**) $C_{64}H_{88}N_{16}O_{24}Cl_3Gd$: C, 44.5; H, 5.1; N, 12.9; O, 22.2; Cl, 6.2; Gd, 9.1. Found: C, 44.5; H, 5.1; N, 12.0; Cl, 5.9; Gd, 8.9. Anal. Calcd **(3)** $C_{68}H_{94}N_{16}O_{23}Cl_3La$: C, 46.7; H, 5.4; N, 12.8; O, 21.0; Cl, 6.1; La, 7.9. Found: C, 44.5; H, 5.3; N, 12.8; Cl, 6.5; La, 7.8. Anal. Calcd (**4**) $C_{68}H_{94}N_{16}O_{23}Cl_3Gd$: C, 46.2; H, 5.4; N, 12.7; O, 20.8; Cl, 6.0; Gd, 8.9. Found: C, 46.0; H, 5.3; N, 12.4; Cl, 5.9; Gd, 8.4.

$[Ln^{III}(NITBzImH)_2(NO_3)_3]$ (5 and 6). Compounds **5** (La) and **6** (Gd) were synthesized as single crystals following the procedure reported here for the gadolinium(III) derivative. To 100 mg (0.22 mmol) of $Gd(NO_3)_3\cdot 6H_2O$ dissolved in 8 mL of ethanol was added 120 mg of **NITBzImH** previously dissolved in 20 mL of ethanol. The resulting solution was slowly evaporated in the air to give after one week 130 mg (66%) of dark blue cubic single crystals. For La and Gd, the yield is, respectively, 69% and 71%. Anal. Calcd for **(5)** $C_{28}H_{34}N_{11}O_{13}La$: C, 38.6; H, 3.9; N, 17.7; O, 23.9; La, 15.9. Found: C, 38.4; H, 4.1; N, 17.3; La, 16.0. Anal. Calcd for **(6)**

(6) Costes, J.-P.; Dahan, F.; Dupuis, A. *Inorg. Chem.* **2000**, *39*, 165.
(7) Bencini, A.; Benelli, C.; Caneschi, A.; Carlin, R. L.; Dei, A.; Gatteschi, D. *J. Am. Chem. Soc.* **1985**, *107*, 8128.
(8) Benelli, C.; Caneschi, A.; Gatteschi, D.; Guilou, L.; Pardi, L. *Inorg. Chem.* **1990**, *29*, 1750.
(9) Benelli, C.; Fabretti, A. C.; Giusti, A. *J. Chem. Soc., Chem. Commun.* **1993**, 409.
(10) Guillou, O.; Bergerat, P.; Kahn, O.; Bakalbassis, E.; Boubeker, K.; Batail, P.; Guillot, M. *Inorg. Chem.* **1992**, *31*, 110.
(11) Andruh, M.; Ramade, I.; Godjovi, E.; Guillou, O.; Kahn, O.; Trombe, J.-C. *J. Am. Chem. Soc.* **1993**, *115*, 1822.
(12) Sanz, J. L.; Ruiz, R.; Gleizes, A.; Lloret, F.; Faus, J.; Julve, M.; Borras-Almenar, J. J.; Journaux, Y. *Inorg. Chem.* **1996**, *35*, 7384.
(13) Costes, J.-P.; Dupuis, A.; Laurent, J.-P. *J. Chem. Soc., Dalton Trans.* **1998**, 735.
(14) Sakamoto, M.; Hashimura, M.; Matsuki, K.; Matsumoto, N.; Inoue, K.; Okawa, H. *Bull. Chem. Soc. Jpn.* **1991**, *64*, 3639.
(15) Matsumoto, N.; Sakamoto, M.; Tamaki, H.; Okawa, H.; Kida, S. *Chem. Lett.* **1990**, 853.
(16) Lescop, C.; Luneau, D.; Belorizky, E.; Fries, P.; Guillot, M.; Rey, P. *Inorg. Chem.* **1999**, *38*, 5472.
(17) Caneschi, A.; Dei, A.; Gatteschi, D.; Sorace, L.; Vostrikova, K. E. *Angew. Chem., Int. Ed.* **2000**, *39*, 246.
(18) Costes, J.-P.; Dahan, F.; Dupuis, A.; Laurent, J.-P. *Inorg. Chem.* **2000**, *39*, 169.
(19) Lescop, C.; Luneau, D.; Bussière, G.; Triest, T.; Reber, C. *Inorg. Chem.* **2000**, *39*, 3740.
(20) Fegy, K.; Luneau, D.; Ohm, T.; Paulsen, C.; Rey, P. *Angew. Chem., Int. Ed.* **1998**, *37*, 1270.
(21) Ullman, E. F.; Osiecky, J. H.; Boocock, D. G. B.; Darcy, R. *J. Am. Chem. Soc.* **1972**, *94*, 7049.

Table 1. Summary of Crystallographic Data for Compounds **1**−**3** and **5**−**6**

	1	**2**	**3**	**5**	**6**
formula	$C_{64}H_{88}Cl_3LaN_{16}O_{24}$	$C_{64}H_{88}Cl_3GdN_{16}O_{24}$	$C_{68}H_{94}Cl_3LaN_{16}O_{23}$	$C_{28}H_{34}LaN_1O_{13}$	$C_{28}H_{34}GdN_1O_{13}$
fw	1710.76	1729.10	1742.80	871.57	889.91
T(K)	143(2)	193(2)	193(2)	298(2)	298(2)
cryst syst	orthorhombic	tetragonal	tetragonal	orthorhombic	orthorhombic
space group	*Fddd*	$P\bar{4}2c$	$P\bar{4}2_1m$	$Pna2_1$	$Pna2_1$
a (Å)	11.0682(8)	16.0682(4)	21.125(3)	19.5002(12)	19.1831(10)
b (Å)	34.240(3)	16.0682(4)	21.125(3)	13.0582(8)	13.1600(7)
c (Å)	42.787(3)	18.7190(6)	10.938(2)	14.5741(9)	14.4107(7)
V (Å^3)	16215(2)	4833.0(2)	4881.5(14)	3711.1(4)	3638.0(3)
Z	8	2	2	4	4
μ (mm^{-1})	0.706	0.837	0.587	1.227	1.900
ρ_{calcd} (cm^3)	1.402	1.188	1.186	1.560	1.625
λ (Å)	0.71073	0.71073	0.71073	0.71073	0.71073
$R(F)^a$ $I > 2\sigma(I)$	0.0876	0.0732	0.1017	0.0331	0.0206
$R_w(F^2)$ all data	0.2336	0.2218	0.3126	0.1146	0.0625

[a] $R(F) = \sum||F_o| - |F_c||/\sum|F_o|$; $R_w(F^2) = \sum[w(F_o^2 - F_c^2)^2/\sum wF_o^4]^{1/2}$.

$C_{28}H_{34}N_{11}O_{13}Gd$: C, 37.8; H, 3.9; N, 17.3; O, 23.4; Gd, 17.7. Found: C, 37.3; H, 3.9; N, 17.0; Gd, 17.2.

X-ray Crystallography. The intensity data for compounds **1**−**3** and **5**−**6** were collected with a Bruker SMART CCD diffractometer equipped with a graphite monochromatized and normal focus molybdenum-target X-ray tube. The data were processed for reduction and absorption through the SAINT software[22] packages, and the structures were solved and refined with the SHELXTL software.[23] All non-hydrogen atoms were refined with anisotropic thermal parameters. The hydrogen atoms were included in the final refinement model in calculated positions with isotropic thermal parameters. Crystal structure and refinement data for compounds **1**−**3** and **5**−**6** are summarized in Table 1.

Magnetic Measurements. A Quantum Design MPMS superconducting SQUID magnetometer was used to measure the temperature dependence of the magnetic susceptibilities of all compounds in the 2−300 K temperature range at a field strength of 0.5 T and to measure the magnetic field dependence of the magnetization in the 0−5.5 T magnetic field range for compounds **2**, **4**, **6** at 2, 4.2, 7, 10 K. For compounds **2** and **4,** the magnetic field dependence of the magnetization were also measured up to 20 T at 4.2 K at the Grenoble High Magnetic Field Laboratory (LCMI-CNRS and Max Planck Institute). The data were corrected for diamagnetism of the constituent atoms.

Results and Discussion

Crystal Structures. Views of the molecular structures for compounds **1**, **3**, and **6** are shown respectively in Figures 2−4. Selected bond lengths are shown in Table 2 for compounds **1**−**3** and in Table 3 for compounds **5**−**6.** Selected inter- and intramolecular distances are displayed in Table 4 for compounds **1**−**3** and **5**−**6**.

In perchlorate salts, the lanthanide ions are eight-coordinated, by four bidentate radicals. Despite different crystalline space groups, compounds **1**−**3** show close structural similarities. All contain crystallization water and THF molecules, so that the complex molecules $[Ln^{III}(radical)_4]^{3+}$ are well magnetically isolated from each other, as is exemplified by Figure 5 in the case of compound **2**. Compound **4** could not be characterized by X-ray crystallography because of the lack of suitable single crystals, but elementary analyses are consistent with the same stoichiometry and the presence of THF and water molecules. Therefore, compound **4** is assumed to be also a gadolinium(III) complex involving four chelating nitronyl nitroxide ligands.

In the case of the nitrate salts, isostructural compounds $[Ln^{III}(radical)_2(NO_3)_3]$ (**5** and **6**) were obtained in which the metal centers are ten-coordinated by two radicals and three nitrato ligands. Complexes **5**−**6** are closely related to those reported by Sutter et al. with a triazole substituted nitronyl nitroxide radical.[5,24]

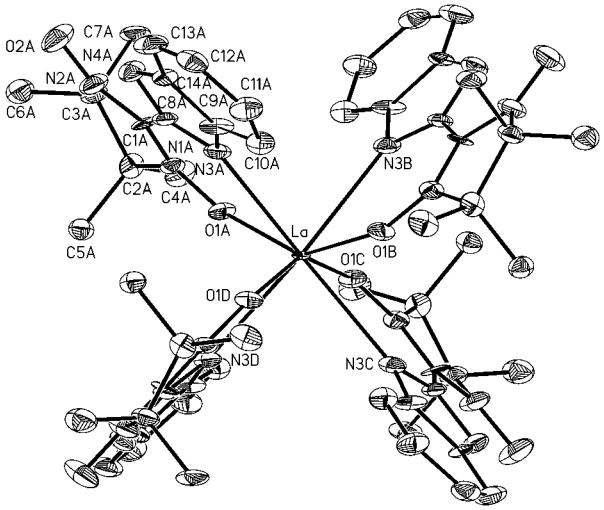

Figure 2. View of the cation $[La^{III}(NITBzImH)_4]^{3+}$ (**1**) with atom labeling and ellipsoids at 30% probability. Hydrogen atoms have been omitted for clarity. (A) *x*, *y*, *z*; (B) −*x*, −*y*, *z*; (C) −*x*, *y*, −*z*; (D) *x*, −*y*, −*z*.

Table 2. Selected Bond Lengths (Å) and Angles (deg) for Complexes **1**−**3**

	1 (Ln = La)	**2** (Ln = Gd)	**3** (Ln = La)
Ln−O1A	2.446(7)	2.352(6)	2.48(2)
Ln−N3A	2.722(7)	2.582(9)	2.68(3)
O1A−N1A	1.29(1)	1.27(1)	1.28(3)
O2A−N2A	1.26(1)	1.27(1)	1.29(3)
O1A−Ln−N3A	68.6(3)	70.4(3)	67.7(9)

(22) *SAINT*, 4.050 ed.; Bruker Analytical X-ray Instruments, Inc.: Madison, WI, 1998.
(23) *SHELXTL*, 5.030 ed.; Brucker Analytical X-ray Instruments, Inc.: Madison, WI, 1998.
(24) Kahn, M. L.; Sutter, J.-P.; Golhen, S.; Guionneau, P.; Ouahab, L.; Kahn, O.; Chasseau, D. *J. Am. Chem. Soc.* **2000**, *122*, 3413.

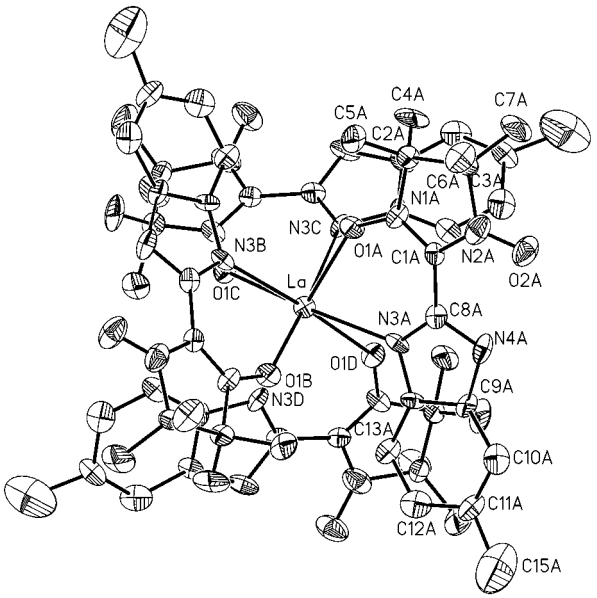

Figure 3. View of the cation $[La^{III}(NITMeBzImH)_4]^{3+}$ (**3**) with atom labeling and ellipsoids at 30% probability. Hydrogen atoms have been omitted for clarity. (A) *x*, *y*, *z*; (B) $-x$, $1 - y$, *z*; (C) $-x$, $-y$, $^1/_2 - z$; (D) *x*, $1 - y$, $^1/_2 - z$.

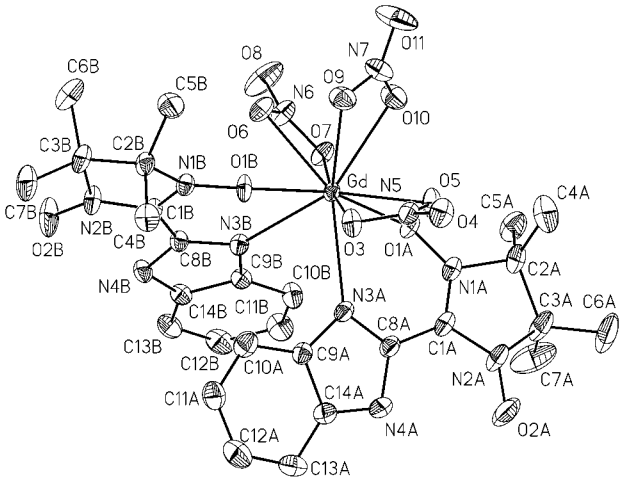

Figure 4. View of complex $[Gd^{III}(NITBzImH)_2(NO_3)_3]$ (**6**) with atom labeling and ellipsoids at 30% probability. Hydrogen atoms have been omitted for clarity. (A and B) *x*, *y*, *z*.

$[La^{III}(NITBzImH)_4]\cdot(ClO_4)_3\cdot 2THF\cdot 2H_2O$ (1). The compound crystallizes in the orthorhombic *Fddd* space group. The unit cell contains 8 $[La^{III}(NITBzImH)_4]^{3+}$ cations, 24 perchlorate anions, 16 molecules of tetrahydrofuran (THF), and 16 molecules of water. A view of the complex cation $[La^{III}(NITBzImH)_4]^{3+}$ is shown in Figure 2. The metal center is surrounded by four nitronyl nitroxide radicals (**NITBzImH**) and is located on the (a, 222) special position. Only one **NITBzImH** radical is needed to describe the coordination sphere, the three others being generated by symmetry operations around the 2-fold axis. The **NITBzImH** radicals coordinate through one oxygen atom of the NO groups (La−O1A, 2.446(7) Å) and through the pyridinyl nitrogen atom of the benzimidazole ring (La−N3A, 2.722(9) Å) (Table 2), so that the coordination number is eight. The analysis of the coordination polyhedron around the lanthanum(III) ion

Table 3. Selected Bond Lengths (Å) and Angles (deg) for Complexes **5** and **6**

	5 (Ln = La)	**6** (Ln = Gd)
Ln−O1A	2.502(4)	2.405(3)
Ln−O1B	2.462(4)	2.365(3)
Ln−N3A	2.731(5)	2.577(3)
Ln−N3B	2.697(5)	2.585(3)
O1A−N1A	1.302(6)	1.291(4)
O1B−N1B	1.282(6)	1.282(4)
O2A−N2A	1.273(7)	1.274(5)
O2B−N2B	1.283(7)	1.274(5)
Ln−O3	2.649(5)	2.577(3)
Ln−O4	2.606(5)	2.506(3)
Ln−O6	2.650()	2.544(3)
Ln−O7	2.624(5)	2.532(3)
Ln−O9	2.591(5)	2.486(3)
Ln−O10	2.590(5)	2.489(3)
O1A−Ln−N3A	68.6(2)	70.9(1)
O1B−Ln−N3B	67.7(1)	70.6(9)

Table 4. Selected Interatomic Distances (Å) for Complexes **1**−**3**, **5** and **6**[a]

	1	**2**	**3**	**5**	**6**
Intramolecular (Coordination Polyhedron)					
O1A···O1B	4.71(1)	3.85(1)	3.95(5)		
O1A···O1C	2.84(1)	2.79(1)	4.10(4)		
O1A···O1D	4.19(1)	4.65(1)	4.10(4)		
O1A···O1B				4.892(6)	4.716(4)
O1A···N3B				3.899(6)	3.724(4)
O1A···N3A	2.92(2)	2.85(1)	2.88(3)		
O1A···N3B	3.59(1)	2.89(1)	3.09(3)		
O1A···N3C	4.74(1)	4.36(1)	5.14(4)		
O1A···N3B	3.10(1)	3.65(1)	2.98(3)		
N3A···N3B	3.58(1)	4.24(2)	4.48(6)		
N3A···N3C	5.33(1)	5.11(2)	4.31(4)		
N3A···N3D	4.24(1)	3.03(2)	4.31(4)		
Intermolecular					
O2A···O2E	4.61(2)	7.01(2)	6.07(5)		

[a] Symmetry operations. **3**: (A) *x*, *y*, *z*; (B) $-x$, $-y$, *z*; (C) $-x$, *y*, $-z$; (D) *x*, $-y$, $-z$; (E) $1 - x$, $-y$, *z*. **5**: (A) *x*, *y*, *z*; (B) $-x$, $-y$, $+z$; (C) $-y$, $-x$, $-z$; (D) $-y$, *x*, $-z$; (E) $^1/_2 - y$, $^1/_2 - x$, *z*. **4**: (A) *x*, *y*, *z*; (B) $-x$, $1 - y$, *z*; (C) $-x$, $-y$, $^1/_2 - z$; (D) *x*, $1 - y$, $^1/_2 - z$; (E) $y - 1$, $-x$, $-z$. **7**, **8**: (A and B) *x*, *y*, *z*.

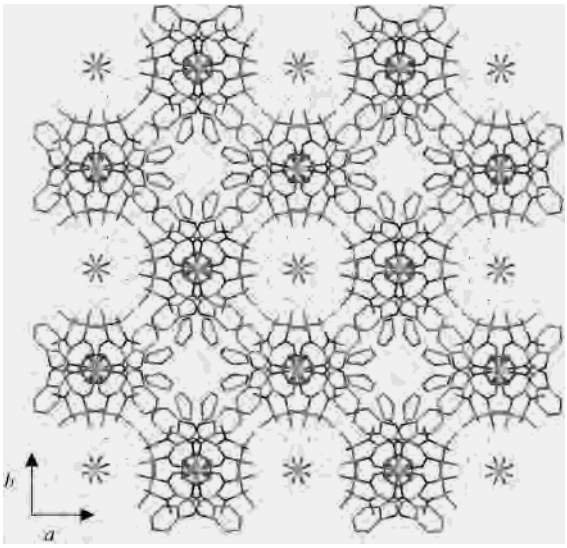

Figure 5. Crystal packing of compound (**2**).

indicates a distortion of the dodecahedron toward a square antiprism (Figure 6).[25,26] The twist angle between the nitronyl nitroxide moiety and the benzimidazolyl substituent is 4.96-

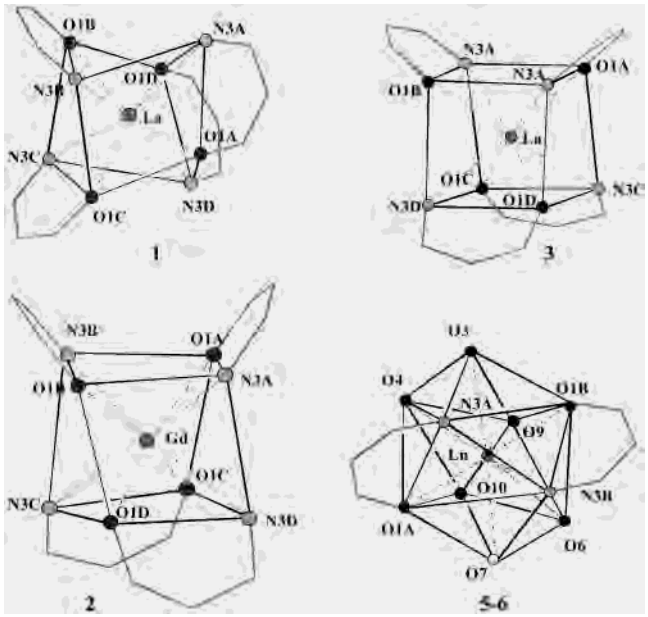

Figure 6. Schematic representation drawn from crystal structure features showing the coordination polyhedron for **1**−**3** and **5**−**6**. For clarity, only the atoms involved in the chelate ring and in the coordination sphere are shown.

(4)°. The shortest separation between the coordinated NO groups involved in the coordination sphere is 2.84(1) Å (Table 4).

In the crystal cell, the perchlorate anions are distributed on two different crystallographic sites. Two-thirds have the chlorine ion (Cl2) located on a 2-fold axis (e, 2 _ _). One-third are disordered with the chlorine ion (Cl1) on the (b, 222) special position, one oxygen atom (O4C) on a 2-fold-axis (e, 2 _ _), and the other oxygen atoms in general position. Therefore, after symmetry operations, the chlorine atom Cl1 exhibits a hexabonded pattern. THF molecules are found on general positions but with statistically half occupied sites. This is in agreement with the fact that occupation of all sites is here forbidden, for it would lead to overlap of the THF molecules. Crystallization water molecules are also located on general positions and were refined with half occupation site. Indeed, the occupation of all the sites is again excluded for it will bring two water molecules in close contact (d < 1.5 Å). The disordered perchlorate anions and the statistically half occupied sites for THF and water molecules may be related through hydrogen bond networks. The main effect of such a crystal packing is to make the $[La^{III}(NITBzImH)_4]^{3+}$ cations fairly well isolated as shown in Figure 5 for complex **2**. The shortest intermolecular distances between two noncoordinated NO groups is 4.61-(3) Å.

$[Gd^{III}(NITBzImH)_4]\cdot(ClO_4)_3\cdot 2THF\cdot 2H_2O$ (2). The compound crystallizes in the noncentrosymmetric tetragonal $P\bar{4}2c$ space group. The unit cell contains two $[Gd^{III}(NITBzImH)_4]^{3+}$ cations, six perchlorate anions, four molecules of tetrahydrofuran (THF), and four molecules of water. A view of the cation $[Gd^{III}(NITBzImH)_4]^{3+}$ was given in our previous communication.[16] The gadolinium(III) ion is surrounded by the four nitronyl nitroxide radicals (**NITBzImH**) and is located on the (d, 222) special position. As for **1**, the four **NITBzImH** radicals of the coordination sphere are symmetry related and coordinate through one oxygen atom of the NO groups (Gd−O1A, 2.352(6) Å) and through the pyridinyl nitrogen atom of the benzimidazole ring (Gd−N3A, 2.582(9) Å) which give an eight coordinated metal center (Table 2). Analysis of the geometrical features shows that the coordination polyhedron is a distorted cube (Figure 6).[25,26] The angle between the nitronyl nitroxide moiety and the benzimidazolyl substituent is 6.84(4)°. The shortest intramolecular distance between the coordinated NO groups within the $[Gd^{III}(NITBzImH)_4]^{3+}$ cation is 3.09(3) Å (Table 4).

The perchlorate anions are distributed on two different crystallographic sites. Two-thirds have the chlorine ion (Cl2) and one oxygen atom (O2C) located on a 2-fold axis [(m, 2 _ _) special position], so that the other three oxygen atoms appear as disordered on six positions with half occupancy of each site. One-third of the perchlorates have the chlorine (Cl1) located on the (b, $\bar{4}$) special position. The crystallization THF and water molecules were well refined considering half site occupancy.

As for **1**, the crystal packing leads to well separated $[Gd^{III}(NITBzImH)_4]^{3+}$ cations as shown in Figure 5. The shortest intermolecular distances between the noncoordinated NO group are more than 6.07(5) Å (Table 4).

$[La^{III}(NITMeBzImH)_4]\cdot(ClO_4)_3\cdot 2THF\cdot 1H_2O$(3). The compound crystallizes in the tetragonal $P\bar{4}2_1m$ space group. The unit cell contains two $[La^{III}(NITMeBzImH)_4]^{3+}$ cations, six perchlorate anions for neutrality, four molecules of tetrahydrofuran (THF), and two molecules of water. A view of the cation $[La^{III}(NITMeBzImH)_4]^{3+}$ is shown in Figure 3. The lanthanum(III) ion, surrounded by the four nitronyl nitroxide radicals (**NITMeBzImH**), has a coordination number of eight and is located on the (a, $\bar{4}$) special positions. As for **1** and **2**, the four **NITMeBzImH** radicals are symmetry related and coordinate in a chelating way (La−O1A, 2.48(2) Å; La−N3A, 2.68(3) Å) (Table 2). The analysis of the structural features of the coordination polyhedron (Figure 6) indicates a distorted cube.[25,26] It is significant to notice that the methyl groups of the benzimidazole moiety are oriented outside the coordination sphere which probably avoids steric hindrance. The shortest separation between the coordinated NO group involved in the coordination sphere is 2.79(1) Å (Table 4). The angle between the nitronyl nitroxide moiety and the benzimidazolyl substituent is 0.90(4)°.

The perchlorate anions are distributed on two different crystallographic sites. Two-thirds have the chlorine ion (Cl2) and two oxygen atoms (O5, O6) located in a mirror (e, _ _m). One-third have the chlorine (Cl1) located on the (b, $\bar{4}$) special position. The THF molecules are located on a mirror (e, _ _m). There are also crystallization water molecules located in special position (2.mm). As already observed for **3** and **4**, the crystal packing allows well separated [La^{III}-

(25) Muetterties, E. L.; Guggenberger, L. J. *J. Am. Chem. Soc.* **1974**, *96*, 1748.
(26) Drew, M. G. B. *Coord. Chem. Rev.* **1977**, *24*, 179.

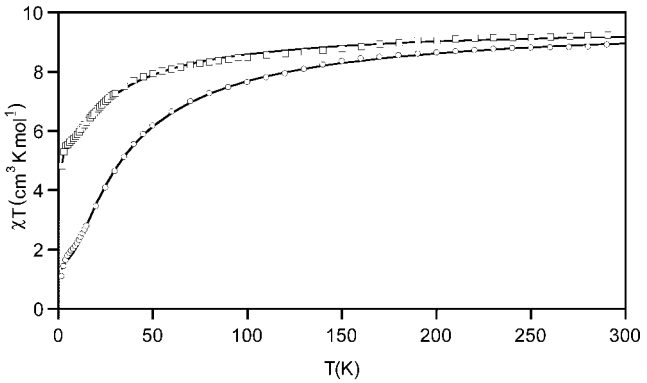

Figure 7. Temperature dependence of χT for compounds $[Gd^{III}(NITBzimH)_4]\cdot(ClO_4)_3\cdot 2THF\cdot 1H_2O$ (**2**) (□) and $[Gd^{III}(NITMeBzimH)_4]\cdot(ClO_4)_3\cdot 2THF\cdot 1H_2O$ (**4**) (○). The solid lines represent the best fit of the data with values in the text for case (ii).

$(NITMeBzImH)_4]^{3+}$ cations, and the shortest intermolecular distances between two noncoordinated NO group are more than 7.01(2) Å (Table 4)

$[Ln^{III}(NITBzImH)_2(NO_3)_3]$ (5, 6). Compounds **5** (La) and **6** (Gd) are isostructural and crystallize in the noncentrosymmetric orthorombic $Pna2_1$ space group. The noncentrosymmetric space group was ascertained by second harmonic generation using the Kurtz and Perry powder test.[27] The $[Ln^{III}(NITBzImH)_2(NO_3)_3]$ complex molecules are shown for the gadolinium complex in Figure 4. The lanthanide ion is ten-coordinated by two chelating nitronyl nitroxide radicals (**NITBzImH**) which are not symmetrically related and three η^2-nitrato anions in a way reminiscent of some bipyridine and phenanthroline lanthanum(III) complexes.[28,29] The differences in bond lengths between the lanthanum complex (La−O1A, 2.502(4) Å; La−O1B, 2.462(4) Å; La−N3A, 2.731(5) Å; La−N3B, 2.697(5) Å) and the gadolinium complex (Gd−O1A, 2.405(3) Å; Gd−O1B, 2.365(3) Å; Gd−N3A, 2.613(3) Å; Gd−N3B, 2.585(3) Å) are in agreement with the lanthanide contraction. The angle between the nitronyl nitroxide moiety and the benzimidazolyl substituent is 17.43° and 7.45° in **5** for radical A and B, respectively, and 17.54° and 8.85° in **6** for radical A and B, respectively. The shortest intermolecular distances are found between the uncoordinated group of the nitronyl nitroxide ligands [O2A···O2Bi, 3.463(9) Å; O2A···N2Bi, 3.503(9) Å and N2A···O2Bi, 3.865(9) Å (**5**)] and [O2A···O2Bi, 3.443(5) Å; O2A···N2Bi, 3.444(5) Å and N2A···O2Bi, 3.832(5) Å (**6**)].

Magnetic Properties. The results are displayed in the form of the product of the magnetic susceptibility with the temperature (χT) in Figure 7 for compounds **2** and **4**, and in Figure 9 for compounds **5**−**6**. The magnetization versus magnetic field is shown in Figure 8 for compounds **2** and **4**, and in Figure 10 for compound **6**.

$[La^{III}(NITBzImH)_4]\cdot(ClO_4)_3\cdot 2THF\cdot 2H_2O$ (1) and $[La^{III}(NITMeBzImH)_4]\cdot(ClO_4)_3\cdot 2THF\cdot 1H_2O$ (3). The χT product is 1.51 cm^3 K mol^{-1} for **1** and 1.57 cm^3 K mol^{-1} for **3** at 300 K. These values are close to those expected for four uncoupled free radicals (1.50 cm^3 K mol^{-1}). Upon cooling, χT keeps practically constant down to 5 K and then decreases abruptly for **3** while for **1** χT is also almost constant down to 20 K, and then it increases slightly reaching a maximum at 3 K (1.64 cm^3 K mol^{-1}) and decreases at lower temperatures. Both behaviors indicate weak radical−radical magnetic interactions which we did not try to quantify.

This is in agreement with weak intermolecular interactions as expected from the crystal structure studies which show well isolated $[Ln^{III}(radical)_4]^{3+}$ units. It also means that the

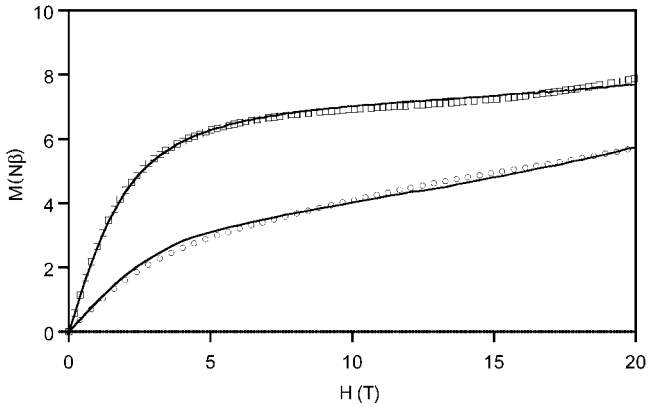

Figure 8. Magnetic field dependence of the magnetization at 2 K for compounds $[Gd^{III}(NITBzimH)_4]\cdot(ClO_4)_3\cdot 2THF\cdot 1H_2O$ (**2**) (□) and $[Gd^{III}(NITMeBzimH)_4]\cdot(ClO_4)_3\cdot 2THF\cdot 1H_2O$ (**4**) (○). The solid lines represent the best fit of the data with values in the text for case (ii).

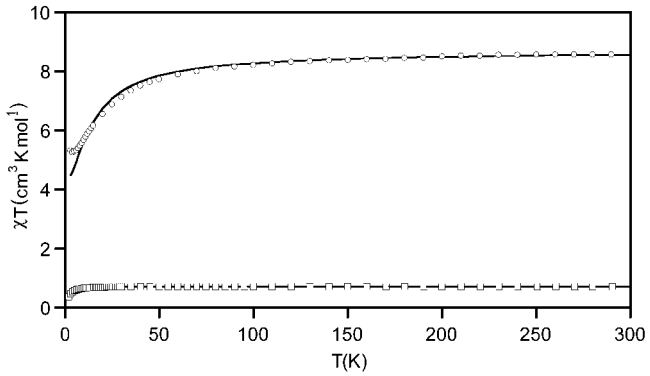

Figure 9. Temperature dependence of χT for compounds $[La^{III}(NITBzImH)_2(NO_3)_3]$ (**5**) (□) and compound $[Gd^{III}(NITBzImH)_2(NO_3)_3]$ (**6**) (○). The solid lines represent the best fit of the data with values in the text.

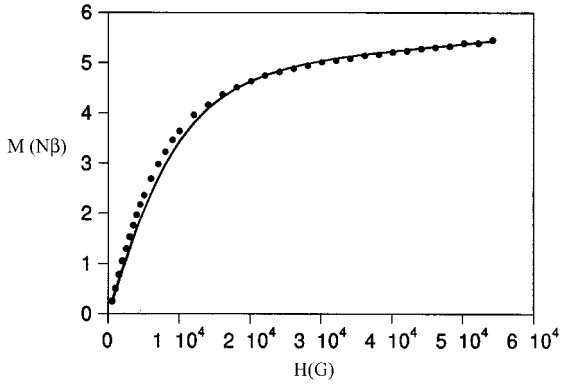

Figure 10. Magnetic field dependence of the magnetization at 2 K for compound $[Gd^{III}(NITBzImH)_2(NO_3)_3]$ (**6**). The solid lines represent the best fit of the data with values in the text.

(27) Kurtz, S. K.; Perry, T. T. *J. Appl. Phys.* **1968**, *39*, 3798.
(28) Al-Karaghouli, A., R.; Wood, J., S. *Inorg. Chem.* **1972**, *11*, 2293.
(29) Fréchette, M.; Butler, I., R.; Hynes, R.; Detellier, C. *Inorg. Chem.* **1992**, *31*, 1650.

intramolecular radical−radical magnetic interactions, operating within the $[Ln^{III}(radical)_4]^{3+}$ units, are moderate.

$[Gd^{III}(NITBzImH)_4]\cdot(ClO_4)_3\cdot 2THF\cdot 2H_2O$ (2) and $[Gd^{III}(NITMeBzImH)_4]\cdot(ClO_4)_3\cdot 2THF\cdot 1H_2O$ (4). χT is 9.45 cm^3 K mol^{-1} for **2** and 9.40 cm^3 K mol^{-1} for **4** at 300 K (Figure 7). These values are close to those expected (9.375 $cm^3\cdot K\cdot mol^{-1}$) for one Gd(III) ($S = {}^7/_2$) and four magnetically independent radicals ($S = {}^1/_2$). Upon cooling, χT decreases continuously for both compounds but faster for **4**. At low temperature (∼5 K) and for both compounds, the χT versus T curves show a shoulder with values close to 5.8 $cm^3\cdot K\cdot mol^{-1}$ for **2** and to 2.0 $cm^3\cdot K\cdot mol^{-1}$ for **4**; then, in both cases, χT falls abruptly at lower temperatures. The field dependence of the magnetization measured at 2 K and in the range 0−5.5 T reaches $7N\,\mu_B$ for **2** and $3N\,\mu_B$ for **4** at 5 T. Measurements up to a magnetic field strength of 20 T show no saturation for compounds **2** and **4** (Figure 8) because of the presence of a large number of spin multiplets (cf. Appendix).

These magnetic behaviors are indicative of dominant antiferromagnetic interactions. From the crystal structure of compounds **1**−**3**, we have seen that the $[Ln^{III}(radical)_4]^{3+}$ species are well separated and should interact loosely. This was confirmed by the magnetic behaviors of lanthanum compounds **1** and **3**. Therefore, to explain the magnetic behaviors of compounds **2** and **4**, we may only consider the Gd^{III}−radical and the radical−radical interactions operating within the $[Gd^{III}(radical)_4]^{3+}$ units. For such a system with spin states ranging between ${}^3/_2$ and ${}^{11}/_2$, the ground spin state $S = {}^3/_2$ observed for **3** indicates unambiguously that the Gd^{III}−radical interactions are antiferromagnetic. The case of compound **2** is not so simple. Indeed, the balance between the Gd^{III}−radical and the radical−radical magnetic interactions may influence the prevalence of a different ground spin state. Such a five spin system was previously studied in detail by Lloret et al. for an oxamido $[Gd^{III}-(Cu^{II})_4]$ complex in which copper(II) is the $S = {}^1/_2$ spin carrier instead of a radical.[12] In that case, the $Gd^{III}-Cu^{II}$ interactions were found to be ferromagnetic. The authors have determined the ground spin states (ranging between ${}^3/_2$ and ${}^{11}/_2$) and the associate temperature dependence of χT as a function of the ratio between the $Cu^{II}-Cu^{II}$ and $Gd^{III}-Cu^{II}$ magnetic interaction either when the latter is ferro- or antiferromagnetic. Following this work, it is impossible to interpret the magnetic data of compound **4**, if the Gd^{III}−radical interactions are assumed to be ferromagnetic.

More precisely, we have interpreted the magnetic properties considering a model with $g = 2$ for all magnetic species, and four Gd^{III}−radical (J_{Gd-rad}) interactions taken as equal, while two possible cases (i and ii) for the nitroxide−nitroxide interactions ($J_{rad-rad}$) were investigated. In the first case (i), the radical−radical magnetic interactions (intramolecular) were considered all equivalent. In the second case (ii), two sets of radical−radical interactions were taken into account. The latter case (ii) was considered on the base of the crystal structure of **2** which shows that in the coordination polyhedron (Figure 6) two O−O distances sets (of the coordinated NO groups) are shorter [O1A−O1C and O1B−O1D, 2.79(1) Å; O1A−O1B and O1C−O1D, 3.85 Å] than the third one [O1A−O1D and O1B−O1C, 4.65(1) Å] (Table 4).

In case (i), we used the following Hamiltonian

$$\mathscr{H} = -2J_{Gd-rad}\mathbf{S}_{Gd}\cdot(\sum_{i=1}^{4}\mathbf{S}_{Gd}\cdot\mathbf{s}_{rad}i) - 2J_{rad-rad}\sum_{\substack{i<j\\ i,j=1}}^{4}\mathbf{s}_{rad}i\cdot\mathbf{s}_{rad}j$$

($\mathbf{s}_{rad}i$ holds for each of the four radicals) as was described previously.[12] With $J_{Gd-rad} < 0$ and $J_{rad-rad} < 0$ (antiferromagnetic interactions), the ground total spin state is $S = {}^3/_2$ for $J_{rad-rad}/J_{Gd-rad} < {}^9/_4$, $S = {}^5/_2$ for ${}^9/_4 < J_{rad-rad}/J_{Gd-rad} < {}^9/_2$, and $S = {}^7/_2$ for $J_{rad-rad}/J_{Gd-rad} > {}^9/_2$ (cf. Appendix). The best fit of the experimental data gave $J_{Gd-rad} = -1.8(3)$ cm^{-1} and $J_{rad-rad} = -7.2(5)$ cm^{-1} with $R = 1.5 \times 10^{-4}$ for **2**, and $J_{Gd-rad} = -3.8$ (2) cm^{-1} and $J_{rad-rad} = -5.6(2)$ cm^{-1} with $R = 1.4 \times 10^{-4}$ for **4** [$R = \Sigma(\chi T_{obs} - \chi T_{calc})^2/\Sigma(\chi T_{obs})^2$].

This means that, for **2**, we have three degenerate ground multiplets $S = {}^5/_2$ with two degenerate multiplets $S = {}^7/_2$ at an energy of only 1.8 cm^{-1}, the next multiplets being at least 10.8 cm^{-1} higher. But in the presence of an external magnetic field H, the lowest Zeeman level is ($S = {}^7/_2$, $M = -{}^7/_2$) for $H > 1.93$ T, which explains the saturation moment at $7\,\mu_B$ at low temperature. On another hand, for **4**, the ground multiplet is $S = {}^3/_2$ which is well separated from the first excited level corresponding to the three degenerate multiplets $S = {}^5/_2$ at an energy 11.8 cm^{-1} above.

In case (ii), we introduced two different radical−radical interactions, $J_1 = J_{rad1-rad3} = J_{rad2-rad4}$ and $J_2 = J_{rad1-rad2} = J_{rad3-rad4}$, and we used the following Hamiltonian:

$$\mathscr{H} = -2J_{Gd-rad}\mathbf{S}_{Gd}\cdot(\sum_{i=1}^{4}\mathbf{s}_{rad}i) - 2J_1(\mathbf{s}_{rad1}\cdot\mathbf{s}_{rad2} + \mathbf{s}_{rad2}\cdot\mathbf{s}_{rad4}) - 2J_2(\mathbf{s}_{rad1}\cdot\mathbf{s}_{rad2} + \mathbf{s}_{rad3}\cdot\mathbf{s}_{rad4})$$

Using this model, the best fit of the experimental data was obtained with $J_{Gd-rad} = -1.7(2)$ cm^{-1}, $J_1 = -6.7(3)$ cm^{-1}, and $J_2 = -4.9(6)$ cm^{-1} with $R = 8.6 \times 10^{-5}$ for **2**, and $J_{Gd-rad} = -3.9(2)$ cm^{-1}, $J_1 = J_2 = -4.9(3)$ cm^{-1} with $R = 1.3 \times 10^{-4}$ for **4**.

In that case, for complex **2**, as in model (i), the lowest multiplet is $S = {}^5/_2$ with a first excited multiplet $S = {}^7/_2$ at 3.3 cm^{-1} and a second excited multiplet $S = {}^3/_2$ at 7.9 cm^{-1}. In the presence of an external field $H > 3.5$ T, the lowest Zeeman level is ($S = {}^7/_2$, $M = -{}^7/_2$), and we find again a saturation moment of $7\,\mu_B$ at low temperature. For complex **4**, the best fit with experiment led to results similar to those obtained with model (i), $J = -3.9$ cm^{-1}, $J_1 = J_2 = -4.9$ cm^{-1}, leading to a ground multiplet ($S = {}^3/_2$) well separated from the first excited level $S = {}^5/_2$ lying at 15.5 cm^{-1}.

We can notice that the two different schemes gave very similar Gd^{III}−radical interactions in both compounds. The reliability of these parameters is strongly supported by the fact that they reproduced perfectly the magnetic field dependence of the magnetization, as shown in Figure 8. Clearly, for compound **2**, model (ii) is more realistic than model (i) according to the crystal structure. For compound **4**, as the structure is not known, it is difficult to predict which

is the most suitable model, and this justified both attempts. Finally, trials to simulate the data considering the Gd^{III}−radical interaction as ferromagnetic were unsuccessful.

$[La^{III}(NITBzImH)_2(NO_3)_3]$ (5). At 300 K, χT is 0.71 $cm^3 \cdot K \cdot mol^{-1}$ (Figure 9) which is close to the value expected for two magnetically independent radicals with spin $S = {}^1/_2$ (0.75 $cm^3 \cdot K \cdot mol^{-1}$). Upon cooling, χT is constant down to 15 K and then decreases continuously. This behavior evidences that weak antiferromagnetic radical−radical interactions operate in the lanthanum complex. One notices that upon cooling the variation of χT versus T is more pronounced in **5** than for the La(radical)$_4$ compounds (**1** and **3**) for which it remains almost constant. This suggests larger antiferromagnetic radical−radical interactions in **5**. The experimental data are well fitted using a dimer model with $g = 1.96$ and $J_{rad-rad} = -1.1$ cm^{-1} ($R = 5.0 \times 10^{-5}$).

Different pathways, either inter- or intramolecular, may be envisaged to account for these radical−radical interactions. However, if we consider the intermolecular distances between the uncoordinated NO groups (>3.4 Å) in compound **5** (as well in **6**), this should lead to negligible intermolecular magnetic interactions: [O2A···O2Bi, 3.443(5) Å; O2A···N2Bi, 3.444(5) Å and N2A···O2Bi, 3.832(5) Å (**8**)]. Indeed, we know from previous works that the coupling between two NO groups relies both on their separation and relative orientations.[30] In **5** (and in **6**), the O−N−C−N−O planes of the two radicals involved in the intermolecular contacts are not parallel (47.63° for **5** and 49.55° for **6**), and their relative orientation (77.77° **5** and $\beta = 79.57°$ for **6**) is unfavorable for strong overlap of the π^* orbitals (perpendicular to the O−N−C−N−O plane of the radical). Another possible pathway for radical−radical interaction is intramolecular such as through the lanthanum metal center as already pointed out.[24]

$[Gd^{III}(NITBzImH)_2(NO_3)_3]$ (6). At 300 K, χT is 8.58 $cm^3 \cdot K \cdot mol^{-1}$ (Figure 9) which is close to the value expected for two radicals and one gadolinium(III) (8.625 $cm^3 \cdot K \cdot mol^{-1}$), magnetically independent. Upon cooling, χT keeps almost constant down to 100 K, and then it decreases continuously and reaches a plateau below 5 K, taking a χT value of 5.5 $cm^3 \cdot K \cdot mol^{-1}$. The magnetic field dependence of the magnetization, measured at 2 K, in the field range 0−5.5 T, tends to saturate at $5N\mu_B$ which corresponds to the expected value for a ground spin state $S = {}^5/_2$.

For such a system with spin states ranging between ${}^5/_2$ and ${}^9/_2$, both the thermal dependence of χT and the field dependence of the magnetization indicate unambiguously that the Gd^{III}−radical interactions are antiferromagnetic which leads to a ground spin state $S = {}^5/_2$. The presence of a plateau in the χT versus T curve clearly indicates that in compound **6** the dominant interactions are the intramolecular ones. Indeed, as was suggested from the crystal structure, the molecular entities [Ln(radical)$_2$(NO$_3$)$_3$] are magnetically well isolated and should interact loosely. Therefore, the interpretation of the magnetic behavior of **6** was performed considering only the Gd^{III}−radical interactions and the intramolecular radical−radical interactions. However, trials to fit the experimental data with only one Gd^{III}−radical coupling constant led to poor results. This is consistent with the fact that the two coordinated radicals are crystallographically independent. Finally, it was possible to fit the magnetic data by taking into account two different antiferromagnetic Gd^{III}−radical interactions ($J_{Gd-rad1}$, $J_{Gd-rad2}$), and one antiferromagnetic intramolecular radical−radical interaction ($J_{rad-rad}$) according to the Hamiltonian

$$\mathscr{H} = -2J_{Gd-rad1}\mathbf{S_{Gd}}\cdot\mathbf{s_{rad1}} - 2J_{Gd-rad2}\mathbf{S_{Gd}}\cdot\mathbf{s}_{rad2} - 2J_{rad1-rad2}(\mathbf{s}_{rad1}\cdot\mathbf{s}_{rad2})$$

The best fit ($R = 5 \times 10^{-3}$) was obtained when fixing the radical−radical interaction at the value found for the isostructural lanthanum complex **5** ($J_{rad1-rad2} = -1.1$ cm^{-1}) and with $J_{Gd-rad1} = -4.05(3)$ cm^{-1} and $J_{Gd-rad2} = -0.80$ cm^{-1}. Importantly, the same set of values reproduces fairly well the dependence of the magnetization with the magnetic field at 2 K (Figure 10).

Conclusion

All gadolinium(III) complexes reported in this paper exhibit antiferromagnetic Gd^{III}−radical interactions. These results and others[17,18] strengthen the idea that ferromagnetism can no longer be considered as an intrinsic property of the Gd^{III}−radical and Gd^{III}−Cu^{II} interaction. From these results, it seems, in opposition with previous convictions, that the Gd^{III}−radical and Gd^{III}−Cu^{II} interaction depends on ligand effects or geometrical parameters. In this context, it is interesting to compare structural parameters in our complexes with those previously obtained for other Gd^{III}−nitroxide complexes. In particularly, Sutter et al. studied a nitrato gadolinium(III) complex structurally close to **6** and found a ferromagnetic Gd^{III}−radical interaction.[5,24] The main significant difference in their gadolinium complex is an elongation of the Gd−O(NO) bond lengths [Gd−O1, 2.460(15) Å and Gd−O4, 2.430(15) Å],[5] compared with those found in ours [Gd−O1A, 2.405(3) Å and Gd−O1b, 2.365(3) Å] for **6** and [Gd−O1A, 2.352(6) Å] for **2** (Tables 3, 4). In other words, in our compounds, the radicals are more tightly bound to the gadolinium(III), and this could be at the origin of the change from ferro- to antiferromagnetic Gd^{III}−radical interaction. Comparison with other gadolinium−nitroxide complexes, which are mainly compounds of the type Gd(hfac)$_3$NITR (hfac = hexafluoroacetylacetonato, R = Ph, i-Pr, and o-Py, p-Py) in which the Gd^{III}−radical interaction is ferromagnetic,[1,3,4] does not evidence such a significant difference. It is possible that in these cases the involved radicals are not chelating and that the electron withdrawing hfac ligands play also a role. This suggests that the sign of the Gd^{III}−radical interaction (ferro or antiferromagnetic) may be governed not only by the donor strength of the radical but by the nature of all the ligands involved in the coordination sphere of the gadolinium. At this point, we are aware that it is not time to propose another model. Indeed, we have to keep in mind that the low spatial extension of

(30) Caneschi, A.; Gatteschi, D.; Sessoli, R.; Rey, P. *Acc. Chem. Res.* **1989**, *22*, 392.

the $4f^7$ orbitals excludes any exchange mechanism between the gadolinium and radical magnetic orbital. In this context, we are now carrying out optical spectroscopy studies on these compounds to gain a better description of their electronic structure.

Acknowledgment. This work was supported in France by the Centre National de la Recherche Scientifique (CNRS), the Commissariat a l'Energie Atomique (CEA), and the Grenoble University (UJF). We thank Dr. M. Guillot for magnetic measurements at the Grenoble High Magnetic Field Laboratory (LCMI-CNRS and Max Planck Institute).

Appendix

The detailed analysis of the various models used for the interpretations of magnetic behavior are given hereafter.

$[Gd^{III}(radical)_2(NO_3)_3]$ (6). The Hamiltonian for a system of one gadolinium(III) with spin **S** ($S = {}^7/_2$) and two nitronyl nitroxide radicals with spins $\mathbf{s_1}$ and $\mathbf{s_2}$ ($s_1 = s_2 = {}^1/_2$) in the presence of an external magnetic field H in the *z* direction is

$$\mathscr{H} = \mathscr{H}_{ex} + \mathscr{H}_{zeeman}$$

The exchange Hamiltonian is given by

$$\mathscr{H}_{ex} = -2a\mathbf{S}\cdot\mathbf{s_1} - 2b\mathbf{S}\cdot\mathbf{s_2} - 2c\mathbf{s_1}\cdot\mathbf{s_2}$$

where *a*, *b*, *c* are the coupling constants $J_{Gd-rad1}$, $J_{Gd-rad2}$, and $J_{rad1-rad2}$, respectively.

The Zeeman Hamiltonian is simply

$$\mathscr{H}_{zeeman} = \mu_B H(g_s S_z + g_1 s_1 z + g_2 s_2 z)$$

The energy levels of $\mathscr{H}_{ex}$ are spin multiplets characterized by the value of the total spin quantum number S_t ($\mathbf{S_t} = \mathbf{S} + \mathbf{s_1} + \mathbf{s_2}$) of the complex and are given by

$$E_1 = E(S_t = {}^5/_2) = (9a + 9b - c)/2$$

$$E_2 = E(\alpha, S_t = {}^7/_2) = [(a + b + c)/2] - \sqrt{X}$$

$$E_3 = E(\beta, S_t = {}^7/_2) = [(a + b + c)/2] + \sqrt{X}$$

$$E_4 = E(S_t = {}^9/_2) = -(7a + 7b + c)/2$$

with $X = 16a^2 + 16b^2 + c^2 - 31ab - ac - bc$.

The molar magnetic susceptibility was derived from the usual expression,[31] assuming $g_s = g_1 = g_2 = g$

$$\chi T = (Ng^2\mu_B 2/3k)\frac{\sum_{S_t} S_t(S_t+1)(2S_t+1)f(S_t)}{\sum_{S_t}(2S_t+1)f(S_t)} \qquad (1)$$

with

$$f(S_t) = \sum_{\alpha}\exp[-E(\alpha, S_t)/kT]$$

where α is used to index the various multiplets corresponding to the same S_t value.

(31) Belorizky, E. *J. Phys. I* **1993**, *3*, 423.

The magnetization was obtained from the relation $M = NkT\,\partial/\partial H \ln Z$, with $Z = \sum_{\alpha,S_t} M\exp[-E(\alpha, S_t, M)]$, $(-S_t \le M \le S_t)$, $E(\alpha, S_t, M)$ being the energy levels of $\mathscr{H}$, that is

$$E(\alpha, S_t, M) = E(\alpha, S_t) + g\mu_B HM$$

In the previous expression, $E(\alpha, S_t)$ is the energy of the multiplets E_i (here, $1 \le i \le 4$).

Finally, we obtain

$$M = (N_i\mu_B g/2)\frac{\sum_{S_t}\{(2S_t+1)\cosh[(2S_t+1)x] - \sinh[(2S_t+1)x]\coth x\}f(S_t)}{\sum_{S_t}[\sinh(2S_t+1)x]f(S_t)} \qquad (2)$$

with $x = (g\mu_B H)/(2kT)$.

For compound **6**, the best fit with experiment was obtained with $g = 2$ and $a = -4.05(3)$ cm^{-1}, $b = -0.80$ cm^{-1}, and $c = -1.1$ cm^{-1}, and the lowest multiplet is $E_1 = E(\mathbf{S_t} = {}^5/_2)$.

$[Gd^{III}(Rad)_4](ClO_4)_3\cdot 2THF\cdot x\mathbf{H_2O}$ (2 and 4). We use the same procedure as that described previously with

$$\mathscr{H}_{zeeman} = g\mu_B H(S_z + \sum_{i=1}^{4} s_{iz})$$

Model (i). The Gd^{III} ion is assumed to interact with four nitronyl nitroxide radicals considered as equivalent. Then

$$\mathscr{H}_{ex} = -2J\mathbf{S}\cdot(\sum_{i=1}^{4}\mathbf{s}_i) - 2J_1\sum_{i<j}\mathbf{s}_i\cdot\mathbf{s}_j$$

where *J* and J_1 are the coupling constants J_{Gd-rad} and $J_{rad-rad}$, respectively. Introducing the total radical spin $\mathbf{S'} = \sum_{i=1}^{4}\mathbf{s}_i$ ($0 \le \mathbf{S'} \le 2$) and the total spin $\mathbf{S_t} = \mathbf{S} + \mathbf{S'}$ of the complex ($^3/_2 \le \mathbf{S_t} \le {}^{11}/_2$), we have

$$\mathscr{H}_{ex} = -2J\mathbf{S}\cdot\mathbf{S'} - J_1\sum_{i=1}^{4}\mathbf{s}_i\cdot(\mathbf{S'} - \mathbf{s}_i) = -J[\mathbf{S_t}^2 - \mathbf{S}^2 - \mathbf{S'}^2] - J_1\mathbf{S'}^2 + J_1\sum_{i=1}^{4}\mathbf{s}_i^2$$

The energy levels are characterized by the quantum numbers S_t and S′. They are given by

$$E(S_t, S') = J[-S_t(S_t+1) + ({}^{63}/_4) + S'(S'+1)] + J_1[3 - S'(S'+1)]$$

More precisely, we get

$$E_1 = E({}^3/_2, 2) = 18J - 3J_1$$

$$E_2 = E({}^5/_2, 2) = 13J - 3J_1$$

$$E_3 = E({}^5/_2, 1) = 9J + J_1 \qquad \text{(3 degenerate multiplets)}$$

$$E_4 = E({}^7/_2, 2) = 6J - 3J_1$$

$$E_5 = E(^7/_2, 1) = 2J + J_1 \qquad \text{(3 degenerate multiplets)}$$

$$E_6 = E(^7/_2, 0) = 3J_1 \qquad \text{(2 degenerate multiplets)}$$

$$E_7 = E(^9/_2, 2) = -3J - 3J_1$$

$$E_8 = E(^9/_2, 1) = -7J + J_1 \quad \text{(3 degenerate multiplets)}$$

$$E_9 = E(^{11}/_2, 2) = -14J - 3J_1$$

With $J < 0$ and $J_1 < 0$ (antiferromagnetic interactions), the ground multiplet is $E_1(S_t = {}^3/_2)$ for $J_1/J < {}^9/_4$, $E_3(S_t = {}^5/_2)$ for ${}^9/_4 < J_1/J < {}^9/_2$, and $E_6(S_t = {}^7/_2)$ for $J_1/J > {}^9/_2$.

The explicit expressions of the susceptibility and magnetization are easily obtained from the preceding levels, using the general formulas 1 and 2.

Taking $g = 2$, the best fit with experiment gave $J = -1.8$ cm^{-1}, $J_1 = -7.2$ cm^{-1}, $J_1/J = 4$ for complex **2** and $J = -3.8$ cm^{-1}, $J_1 = -5.6$ cm^{-1}, $J_1/J = 1.47$ for complex **4**.

This shows that for **2**, we have three degenerate ground multiplets $E_3(\mathbf{S}_t = {}^5/_2)$ with two degenerate multiplets $E_6(\mathbf{S}_t = {}^7/_2)$ at energy of only 1.8 cm^{-1}, the next multiplets being at least 10.8 cm^{-1} higher. But in the presence of an external magnetic field H, the lowest Zeeman level is $E_6(\mathbf{S}_t = {}^7/_2, M = -{}^7/_2)$ for $H > 1.93$ T, which explains the saturation moment at 7 μ_B at low temperature. On another hand, for **4**, the ground multiplet is $E_1(S_t = {}^3/_2)$ which is well separated from the first excited level corresponding to the three degenerate multiplets $E_3(S_t = {}^5/_2)$ at an energy 11.8 cm^{-1} above.

Model (ii). We introduce two different radical−radical interactions, $J_{rad1-rad3} = J_{rad2-rad4} = J_1$, $J_{rad1-rad2} = J_{rad3-rad4} = J_2$, and we neglect $J_{rad1-rad4}$ and $J_{rad2-rad3}$

In **2**, J_1, J_2, and the neglected exchange interaction correspond to radical−radical distances (O−O) of 2.79, 3.85, and 4.65 Å, respectively (Figure 6 and Table 4).

Then

$$\mathcal{H}_{ex} = -2J\mathbf{S}\cdot\mathbf{S}' - 2J_1(\mathbf{s_1}\cdot\mathbf{s_3} + \mathbf{s_2}\cdot\mathbf{s_4}) - 2J_2(\mathbf{s_1}\cdot\mathbf{s_2} + \mathbf{s_3}\cdot\mathbf{s_4}) \quad (3)$$

with $\mathbf{S}' = \sum_{i=1}^{4} \mathbf{s}_i$. The terms involving J_1 and J_2 do not commute. However, as S′ commutes with these terms, S′ is a good quantum number, and setting $\mathbf{S}_t = \mathbf{S} + \mathbf{S}'$, the various multiplets are still partly characterized by S_t and S′. The energy levels $\mathbf{E}_i(S_t, S')$, where the index i is used to label the different multiplets corresponding to the same S_t and S′ values, are readily obtained after direct diagonalization of the sum of the two last terms in eq 3 and are given by

$$E_1 = E(^3/_2, 2) = 18J - J_1 - J_2$$

$$E_2 = E(^5/_2, 2) = 13J - J_1 - J_2$$

$$E_3 = E_1(^5/_2, 1) = 9J + J_1 + J_2$$

$$E_4 = E_2(^5/_2, 1) = 9J + J_1 - J_2$$

$$E_5 = E_3(^5/_2, 1) = 9J - J_1 + J_2$$

$$E_6 = E(^7/_2, 2) = 6J - J_1 - J_2$$

$$E_7 = E_1(^7/_2, 1) = 2J + J_1 + J_2$$

$$E_8 = E_2(^7/_2, 1) = 2J + J_1 - J_2$$

$$E_9 = E_3(^7/_2, 1) = 2J - J_1 + J_2$$

$$E_{10} = E_1(^7/_2, 0) = J_1 + J_2 - 2\sqrt{J_1^2 + J_2^2 - J_1J_2}$$

$$E_{11} = E_2(^7/_2, 0) = J_1 + J_2 + 2\sqrt{J_1^2 + J_2^2 - J_1J_2}$$

$$E_{12} = E(^9/_2, 2) = -3J - J_1 - J_2$$

$$E_{13} = E_1(^9/_2, 1) = -7J + J_1 + J_2$$

$$E_{14} = E_2(^9/_2, 1) = -7J + J_1 - J_2$$

$$E_{15} = E_3(^9/_2, 1) = -7J - J_1 + J_2$$

$$E_{16} = E(^{11}/_2, 2) = -14J - J_1 - J_2$$

The molar susceptibility and magnetization were calculated through eqs 1 and 2 with $g = 2$. For complex **2**, the best fit was obtained with $J = -1.7$ cm^{-1}, $J_1 = -6.7$ cm^{-1}, and $J_2 = -4.9$ cm^{-1}. As in model (i), the lowest multiplet is $E_3(S_t = {}^5/_2)$ with a first excited multiplet $E_{10}(S_t = {}^7/_2)$ at 3.3 cm^{-1} and a second excited multiplet $E_1(S_t = {}^3/_2)$ at 7.9 cm^{-1}. In presence of an external field $H > 3.5$ T, the lowest Zeeman level is $E_{10}(S_t = {}^7/_2, M = -{}^7/_2)$, and we find again a saturation moment of 7 μ_B at low temperature.

For complex **4**, the best fit with experiment led to results similar to those obtained with model (i): $J = -3.9$ cm^{-1}, $J_1 = J_2 = -4.9$ cm^{-1} leading to a ground multiplet $E_1(S_t = {}^3/_2)$ well separated from the first excited level $E_3(S_t = {}^5/_2)$ lying at 15.5 cm^{-1}.

Supporting Information Available: Crystallographic data for compounds **1**−**3** and **5**−**6** are available in CIF format. This material is available free of charge via the Internet at http://pubs.acs.org.

IC0200038